Force field inside the void in complex plasmas under microgravity conditions

M. Kretschmer, S. A. Khrapak, S. K. Zhdanov, H. M. Thomas, and G. E. Morfill
Centre for Interdisciplinary Plasma Science, Max-Planck-Institut für extraterrestrische Physik, D-85741 Garching, Germany

V. E. Fortov, A. M. Lipaev, and V. I. Molotkov
Institute for High Energy Densities, Russian Academy of Sciences, Izhorskaya 13/19, 125412 Moscow, Russia

A. I. Ivanov and M. V. Turin
RSC "Energia" Korolev, 141070 Moscow Region, Russia
(Received 13 December 2004; published 2 May 2005)

Observations of complex plasmas under microgravity conditions onboard the International Space Station performed with the Plasma-Kristall experiment-Nefedov facility are reported. A weak instability of the boundary between the central void (region free of microparticles) and the microparticle cloud is observed at low gas pressures. The instability leads to periodic injections of a relatively small number of particles into the void region (by analogy this effect is called the "trampoline effect"). The trajectories of injected particles are analyzed providing information on the force field inside the void. The experimental results are compared with theory which assumes that the most important forces inside the void are the electric and the ion drag forces. Good agreement is found clearly indicating that under conditions investigated the void formation is caused by the ion drag force.

DOI: 10.1103/PhysRevE.71.056401 PACS number(s): 52.27.Lw, 52.35.−g

I. INTRODUCTION

The Plasma-Kristall experiment (PKE)-Nefedov facility [1] onboard the International Space Station (ISS), operational since March 2001, has enabled the study of complex (dusty) plasmas under microgravity conditions. A complex plasma is generated by introducing micron sized particles (grains) in a capacitively coupled radio frequency (rf) discharge. The grains form a cloud inside the bulk of the discharge and can be easily visualized with the help of standard tools—laser illumination and CCD video cameras. Some of the experimental results on complex plasmas under microgravity conditions were reported recently, including formation of localized crystalline structures [1], investigations of complex plasma boundaries [2,3], grain component transport properties [4,5], excitation and analysis of low-frequency waves [6,7], observation of dust-acoustic shocks [8], decharging of complex plasma [9], and the observation of the so-called "heart-beat" instability [10].

In most of the experiments under microgravity conditions the central region of the discharge is free of grains—a so-called "void" is formed. The void is formed over a broad range of complex plasma parameters [1–11]. It is also observed in ground-based experiments with relatively small (growing) particles [12,13] or when applying an additional external force (e.g., thermophoresis) to compensate for gravity [14–16], so that the grain component can levitate in the bulk of the discharge. Due to recent theoretical advances, showing that the ion drag force can be more than a factor of ten larger than had traditionally been believed, void formation is now thought to be a consequence of this (enhanced) interaction [17]. The way this process works is the following: momentum is transferred from the ions drifting from the central region of a discharge to its walls and electrodes. The ion drag force pushes the grains from the the center and a void will form if it exceeds the electric force (which acts in the opposite direction for the negatively charged particles). Other models of the void formation have also been proposed based, e.g., on the thermophoretic force [11] and "plasma holes" [18,19], etc. So far no direct experimental results were reported providing a clear picture of the nature of the void formation.

The void structure is usually stable, but for certain complex plasma parameters the void-complex plasma interface experiences oscillations, typically with a frequency of a few Hz [10,13], accompanied by a perturbation of the complex plasma cloud. This effect is known as "heart-beat" instability, because the grains exhibit a throbbing motion such as a muscle in a heart [10]. The origin of this instability is under active investigation [20].

In this paper we report on the observation of a weak instability of the void-complex plasma interface observed at a relatively low gas pressure ($p=12$ Pa). The observed instability is accompanied by periodic "contractions" of the void volume and fast injection of grains into the void region. In the next "expansion" stage the injected grains are pushed back into the complex plasma cloud and a (metastable) void structure reestablishes itself. The whole cycle repeats periodically. In many ways the observed instability is similar to the heart-beat instability, however, it has some important distinctive features: the complex plasma cloud is only weakly perturbed during the instability (the perturbation seems to be confined to the surface layer only) and a relatively small number of grains is injected from the interface into the void. Hence the void structure is almost unaffected by the instability—in contrast to the heart-beat instability where the void is practically filled with particles during the instability cycle. For this reason we believe that the observed effect can be distinguished from the heart-beat instability [21].

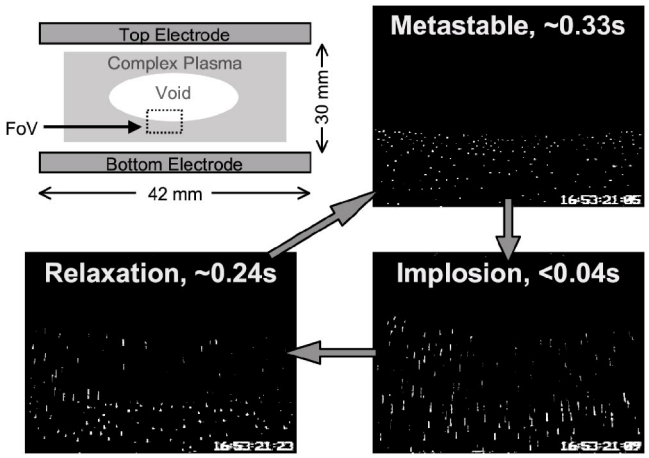

FIG. 1. Sketch of experimental geometry (top left); particle cloud, preelectrode sheaths, and central void (area free of grains) are shown schematically. The field of view (FoV) of the "high resolution camera" is indicated, too. The figure also shows repeating stages of the "trampoline" instability: The metastable interface layer (top right) containing small charged grains is pushed out periodically into the void region (fast "implosion phase," bottom right), and then relaxes ("relaxation" stage, bottom left) back to the metastable equilibrium.

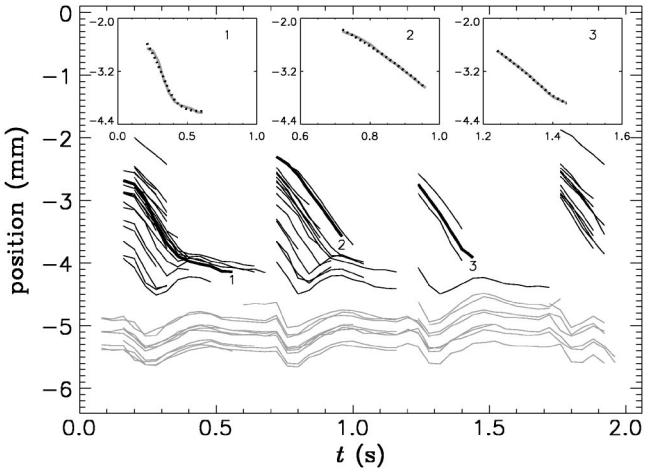

FIG. 2. 71 digitized grain trajectories during four consecutive instability cycles. Dark (gray) curves correspond to small (large) grains. The inserts (dotted lines) show fits to three representative experimental trajectories (bold solid lines marked 1, 2, and 3) with an analytical solution of the grain's equation of motion. The analytical solution uses the potential energy inside the void given by Eq. (2) and initial conditions $x(0)=x_0$ and $V(0)=0$.

The expansion (relaxation) stage is relatively slow, which allows us to trace accurately the grain trajectories inside the void. From this analysis the total force acting on the grains and the potential energy profile inside the void are reconstructed. For the relatively low neutral gas pressure used in the experiment a direct comparison with theory involving a model of the ion drag force in the collisionless regime is possible. Such a comparison yields good agreement, implying that we have observed the first experimental confirmation of the ion drag mechanism as being responsible for the void formation in complex plasmas.

II. EXPERIMENTAL SETUP

The PKE-Nefedov facility consists of a plasma chamber with all electronic and mechanical parts integrated into a single barrel-shaped experiment container [1]. The experiments are conducted remotely from a "telescience unit," that mainly contains a laptop computer for controlling the experiment parameters and two video tape recorders for storing the resulting video data. The plasma chamber consists of a glass box with two circular electrodes with a diameter of 4.2 cm separated by a distance of 3 cm. The rf discharge is generated in argon at a frequency of 13.56 MHz and a voltage up to 50 V. The grains (Melamine-Formaldehyde spheres) injected into the chamber are illuminated by a laser sheet of thickness approximately 100 μm. Two cameras are looking into the discharge volume with a field of view of 28.2×21.2 mm^2 ("overview") and 8.55×6.5 mm^2 ("high resolution"), each with a rate of 25 frames per second. For the high resolution camera the pixel resolution is 11.8 μm/pixel. Both camera signals are recorded to video tapes. A schematic view of the experimental setup is shown in Fig. 1, more details can be found in Ref. [1].

The experiment described in this paper is conducted with a rf voltage of 21 V at a relatively low neutral gas pressure of 12 Pa. Grains of 1.7 and 3.4 μm radius are used. The grains of different sizes do not mix, they separate in two clouds. The smaller grains form a thin layer at the edge of the void, larger grains are located further out. In Fig. 1 the smaller grains can be easily identified due to their smaller separation distances (during the metastable state). They are located above the larger grains. The interparticle distances are found to be 157 ± 26 μm between small grains and 275 ± 44 μm between large grains.

III. TRAMPOLINE EFFECT

In the experiments periodic disturbances of the void-complex plasma interface are observed. These self-excited disturbances correspond to a weak instability of the interface, the origin of which we will not discuss in the present paper. The layer of smaller grains is mainly affected by the instability, the larger grains are only weakly perturbed (see Fig. 2). The instability cycle can be separated into three stages: metastable, implosion, and relaxation (expansion) stages (see Fig. 1). During the metastable stage, which is visibly "stable" during a relatively long time ($\sim$0.33 s), the void slowly grows and the layer of smaller grains is slightly compressed. It seems that at this stage the cloud stores the potential energy.

When the energy stored becomes large enough to switch on the instability, a very fast "implosion," with a duration less than $\frac{1}{25}$ s (exposure time) occurs. As a result, the small grains penetrate into the void to a distance up to $\sim$3 mm, which is more than one order of magnitude larger than the intergrain separation inside the cloud.

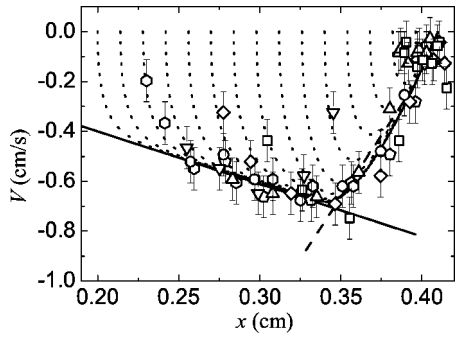

FIG. 3. Grain vertical velocity V versus vertical coordinate x for seven representative trajectories (marked by different symbols). Solid and dashed lines correspond to constant slopes of $V(x)$ where the measurements seem to concentrate. The dotted lines correspond to analytical solutions of the equation of motion with the potential energy inside the void given by Eq. (2) and different initial positions inside the void. The initial grain velocity is zero in these calculations. The error bars for the measured grain velocity are due to the uncertainty in grain position associated with finite resolution.

The fast implosion stage is followed by a relaxation stage: Grains return into the cloud and the metastable state is reestablished. The sum of the forces must be such that the grains are pushed from the central part of the void region. In addition, moving grains are slowed down by the neutral gas drag force. Since the number density of grains in the (previous) void region is too small for collective effects to occur, these grains individually test the force field inside the void. The relaxation is a relatively slow process, it takes $\Delta t \sim 0.24$ s. It is important to note that this time is much longer than the time scale for the damping due to neutral gas $\nu_{dn}^{-1} \sim 0.02$ s, for our experimental conditions.

IV. TRAJECTORY ANALYSIS

To analyze the grain trajectories during the expansion stage a (high resolution) video of duration of 2.3 s is digitized and grain positions in consecutive frames are identified and their trajectories are followed through the video sequence. A total amount of 71 trajectories at four consecutive expansion stages are traced (Fig. 2). It is convenient to proceed with the analysis in two steps. First, we plot a (V,x) diagram for several representative grain trajectories (Fig. 3), where V is the vertical (x) component of the grain velocity. This diagram allows us to make preliminary assumptions concerning the form of the potential energy distribution inside the void. Figure 3 shows that experimentally obtained $V(x)$ data cluster near two lines with constant slopes of different signs. The physical interpretation is that in the central region of the void the total (repulsive) force increases with distance from the center and accelerates the grains ($dV/dx > 0$), whereas closer to the void boundary the force decreases and even changes sign, so that the grains are decelerated ($dV/dx < 0$). For the experimental conditions the inertia term in the grain equation of motion

$$\frac{dV}{dt} + \nu_{dn} V = \frac{F}{M}, \tag{1}$$

can be neglected to a first approximation when analyzing grain motion during the relaxation stage. (Here F is the total force acting on the grain, $\nu_{dn} \simeq 42\ \mathrm{s}^{-1}$ is the characteristic damping rate due to dust-neutral collisions, assuming diffuse scattering with full accommodation, and M is the grain mass.) This can be seen quite easily: the characteristic grain velocity inside the void $V \sim 0.5$ cm/s changes considerably during the relaxation stage ($\Delta t \sim 0.2$ s) so that $dV/dt \sim V/\Delta t \ll \nu_{dn} V$. Hence the grain velocity is proportional to the local force field inside the void $V(x) \simeq F(x)/M\nu_{dn}$. The constant slopes of the $V(x)$ dependence imply that the total force is linear on the coordinate. This gives us an idea how to approximate the potential energy structure inside the void. A reasonable approximation would be two matched parabolas

$$U(r) = \begin{cases} -\frac{1}{2} k_1 x^2, & x \leqslant x_*, \\ \frac{1}{2} k_2 (L-x)^2 - U_0, & x > x_*. \end{cases} \tag{2}$$

Matching of the potential and its derivative (force) at $x = x_*$ yields $x_* = [k_2/(k_1+k_2)]L$ and $U_0 = \frac{1}{2}[k_1 k_2/(k_1+k_2)]L^2$. The potential structure given by Eq. (2) contains three free parameters k_1, k_2, and L. Physically k_1 and k_2 correspond to the constant slopes of the $V(x)$ dependence while L is the position of the potential energy minimum (zero force). The energy U_0 corresponds to the height of the potential barrier between the void center and the boundary. The position of the potential energy minimum L should approximately correspond to the position of the void-complex plasma interface.

In a second step we use the functional form of expression (2) to find the accurate values of the parameters k_1, k_2, and L. Equations (1) and (2) are solved analytically with respect to $x(V = dx/dt)$, keeping the inertia term and with the initial conditions $x(0) = x_0$ and $V(0) = 0$. The solution is fitted to the experimental trajectories. (Three examples of such a fit are shown as inserts in Fig. 2.) The parameters k_1, k_2, and L are found using a least square minimization procedure. To have good statistics all the trajectories shown in Fig. 2 by black lines are employed for the analysis. The results are presented in Fig. 4. We find $k_1 \simeq 7800 \pm 200$ eV/cm^2, $k_2 \simeq 1660 \pm 50$ eV/cm^2, and $L = 0.40 \pm 0.01$ cm. This also yields $U_0 \simeq 110$ eV, and $x_* \simeq 0.33$ cm. The resulting potential energy distribution is shown in Fig. 5 by the solid line.

V. DISCUSSION

To compare the experimental findings with the theoretical predictions we assume that the grains inside the void are mostly affected by the electric force F_E and the ion drag force F_i. The qualitative picture of the void formation is the following: In the central part of the discharge the electric field is weak and the ion drift is subthermal. The electric force scales as $F_E \propto E$, while the ion drag force scales as $F_i \propto v_i \propto E$, where v_i is the ion drift velocity. The ratio F_i/F_E is thus independent of the electric field. Under the condition $|F_i/F_E| = \mathrm{const} > 1$, the individual grains are pushed out of the center and a void is formed. The electric field increases from the center to the periphery, and so does the ion drift velocity. For suprathermal drifts ($v_i > v_{T_i}$) the drift velocity

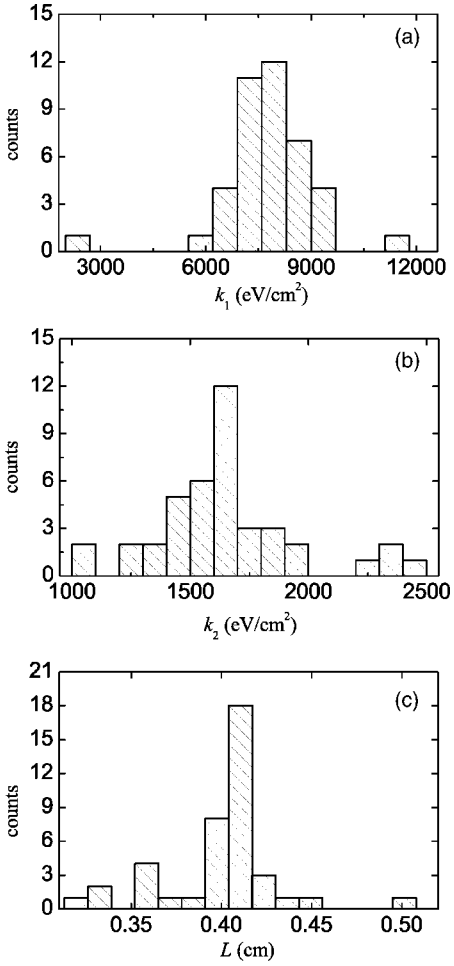

FIG. 4. The fit parameters k_1 (a), k_2 (b), and L (c) of the potential energy distribution modeled by two matched parabolas [Eq. (2)]. The results are obtained by fitting the experimental grain trajectories with the analytical solution of the grain equation of motion. The values of k_1, k_2, and L are determined from a least square minimization procedure.

scales with the electric field as $v_i \propto \sqrt{E}$ and the ion drag force scales as $F_i \propto v_i^{-2} \propto E^{-1}$ [23]. Therefore the ratio $|F_i/F_E|$ decreases fast in this regime and at some point the balance condition $|F_i| = |F_E|$ is achieved. This point corresponds to the stable equilibrium for an individual grain (i.e., to the potential energy minimum) and characterizes the position of the void boundary.

Let us proceed to the quantitative analysis. The electric force acting on the grain is

$$F_E = ZeE, \tag{3}$$

where Z is the grain charge number. The neutral gas pressure is sufficiently low in the experiment so that we can apply the existing theory for the ion drag force in the collisionless regime for the ions. The assumption of "individual" particles is also well justified for the grains whose trajectories are analyzed. An expression for the ion drag force for this case which is applicable for arbitrary ion drift velocity is derived in Refs. [22,23]

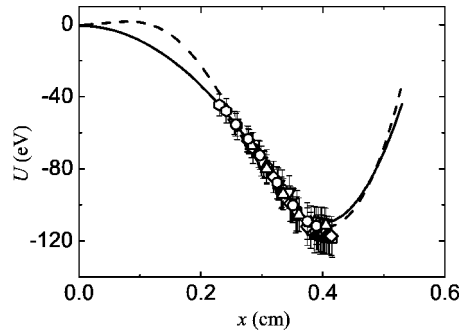

FIG. 5. Potential energy distribution inside the void. The solid line corresponds to the experimental results [form of Eq. (2) with the fitting parameters determined from the analysis of all data]. Symbols correspond to the representative trajectories displayed in Fig. 2, error bars are due to uncertainties in grain position, velocity, and fitting parameters for the potential energy. The dotted line is calculated from theory. The free parameter in this calculation is the derivative of the electric field in the central part of an rf discharge. This was taken to be $E' \simeq 10$ V/cm^2 to achieve agreement with the experimental results.

$$F_i = \sqrt{2\pi} a^2 n m v_{T_i}^2 \left\{ \sqrt{\frac{\pi}{2}} \mathrm{erf}\left(\frac{u}{\sqrt{2}} \right) [1 + u^2 + (1 - u^{-2})(1 + 2z\tau) + 4z^2\tau^2 u^{-2} \ln \Lambda] + u^{-1}[1 + 2z\tau + u^2 - 4z^2\tau^2 \ln \Lambda] \times \exp\left(-\frac{u^2}{2} \right) \right\}, \tag{4}$$

where a is the grain radius, n is the plasma number density, m is the ion mass, $u = v_i/v_{T_i}$ is the ion drift velocity normalized to the ion thermal velocity, $v_{T_i} = \sqrt{T_i/m}$, $z = |Z|e^2/aT_e$ is the normalized grain charge number, and $\tau = T_e/T_i$ is the electron-to-ion temperature ratio. The Coulomb logarithm $\ln \Lambda$ is given by [17,23]

$$\ln \Lambda = \ln\left[\frac{\beta + 1}{\beta + (a/\lambda)} \right], \tag{5}$$

where $\beta \simeq [z\tau/(1+u^2)](a/\lambda)$ is the so-called scattering parameter and λ is the (ion drift velocity dependent) effective screening length. As shown in Ref. [23] a reasonable approximation for $\lambda(u)$ is

$$\lambda(u) = [\lambda_{Di}^{-2}(1 + u^2)^{-1} + \lambda_{De}^{-2}]^{-1/2}, \tag{6}$$

where $\lambda_{Di(e)} = \sqrt{T_{i(e)}/4\pi e^2 n}$ is the ion (electron) Debye radius. It exhibits the following asymptotic behavior: in an isotropic plasma (subthermal ion flows, $u \ll v_{T_i}$) the screening length is given by the linearized Debye radius, while for highly suprathermal flows ($u \gg v_{T_i}$) the ions cannot participate in the screening and $\lambda = \lambda_{De}$. Equation (5) for the Coulomb logarithm is applicable for linear and weakly nonlinear regimes of ion-grain coupling $\beta \lesssim 5$ [17]. In our conditions the maximum value of $\beta \simeq 2$ is achieved at $u = 0$.

Using Eqs. (3) and (4) we compare the experimentally reconstructed profile of the potential energy inside the void with the theoretical one. In doing so we neglect the interaction between the grains—this effect can only be important in

a relatively narrow region close to the void-complex plasma interface. We also assume that in the vicinity of the discharge center the electric field grows linearly with position x, i.e., $E(x)=E'x$. Then the potential energy can be calculated via

$$U(x) = -\frac{1}{E'}\int_0^{E'x} [F_i(\xi) + F_E(\xi)]d\xi, \tag{7}$$

where $F_i(E)$ and $F_E(E)$ are given by Eqs. (3) and (4), respectively. The dependence of the ion drag force on the electric field E comes from the dependence of the drift velocity v_i on E. The latter is assumed mobility limited, i.e., $v_i=\mu E$. We use the approximation of Frost [24] for argon ion mobility in argon gas $\mu(E)=\mu_0 p^{-1}[1+\alpha(E/p)]^{-1/2}$, where $\mu_0 = 1460\ \mathrm{cm}^2/\mathrm{V\,s}$, p is the pressure in Torr, and $\alpha = 0.0264\ \mathrm{cm/V}$. We also assume the following plasma parameters: $T_i \sim T_n \sim 0.025$ eV, $T_e \sim 2$ eV, $n_e \sim n_i \sim 10^9\ \mathrm{cm}^{-3}$. The grain charge in complex plasma under microgravity conditions was recently estimated by exciting low frequency waves in the particle cloud and fitting the obtained dispersion relations with the theoretical ones. The resulting dimensionless charges found from these experiments ranges from $z \sim 0.4$ [6] to $z \sim 0.8$ [7], which is considerably smaller than the collisionless orbital motion limited (OML) theory predicts $z_{\mathrm{OML}} \sim 2$. Similar charge reduction compared to the OML theory was recently observed in experiments by Ratynskaia *et al.* [25]. Such a difference can be attributed to the effect of ion-neutral collisions which can significantly affect charging even when the ion mean free path is longer than the plasma screening length [26–28]. For this reason in the present paper we assume a constant value of the dimensionless charge $z=0.6$, which is believed to be accurate to within approximately 50%.

The potential calculated from Eq. (7) for the complex plasma parameters given above is shown in Fig. 5. The agreement with the potential energy distribution derived experimentally from the trampoline effect (from ~ 0.2 to ~ 0.4 cm from the void center) is very good.

Thus, our results support the assumption that the ion drag force is responsible for the formation of the void in complex plasma under microgravity conditions, at least for the parameter range investigated. The analysis of other experimental observation (e.g., at higher pressures and/or with larger particles) requires an adequate model for the ion drag force, which takes into account simultaneously both nonlinear coupling between the ions and the grains and ion-neutral collisions. So far only models that describe either weakly and strongly nonlinear (as well as linear) collisionless regimes [17,29,30] or linear collisional regime [31–33] are available.

To conclude this section we give some numbers characterizing the void under the conditions investigated: The height of the potential energy barrier between the void center and boundary is $U_0 \sim 110$ eV, the half-width of the void in the vertical direction is ~ 0.4 cm, the electric field and the normalized ion drift velocity close to the void boundary is $E \sim 4\ \mathrm{V/cm}$ and $u \sim 2.5$, respectively.

VI. CONCLUSION

In this paper we reported an observation of the instability of the microparticle cloud-void interface. The instability was accompanied by periodic contractions of the void volume and fast injection of a relatively small number of dust grains into the void region. In the subsequent relaxation stage the injected grains were pushed from the void back into the particle cloud and the void reformed. The relaxation stage was slow enough so that an accurate analysis of grain trajectories was possible. From this analysis the force field and the potential energy distribution inside the void region were reconstructed. Due to the relatively low neutral gas pressure used in the experiments a direct comparison with theory, which uses a model of the ion drag force developed for collisionless ions, was possible. Such a comparison was performed and good agreement between theoretical and experimental results was found. The results support the ion drag mechanism of the void formation in complex plasmas under microgravity conditions.

ACKNOWLEDGMENTS

This work was supported by DLR/BMBF Grant No. 50WM9852 and by the Presidium of the Russian Academy of Sciences under the program "Thermophysics and Mechanics of Extreme Power Impacts." The authors appreciate valuable comments of Dr. U. Konopka and acknowledge the excellent support of the PKE-Nefedov team (see Ref. [1]).

[1] A. Nefedov *et al.*, New J. Phys. **5**, 33 (2003).
[2] B. M. Annaratone *et al.*, Phys. Rev. E **66**, 056411 (2002).
[3] P. M. Bryant, New J. Phys. **6**, 60 (2004).
[4] V. E. Fortov *et al.*, Phys. Rev. Lett. **90**, 245005 (2003).
[5] V. E. Fortov *et al.*, JETP **96**, 704 (2003).
[6] S. A. Khrapak *et al.*, Phys. Plasmas **10**, 1 (2003).
[7] V. V. Yaroshenko *et al.*, Phys. Rev. E **69**, 066401 (2004).
[8] D. Samsonov *et al.*, Phys. Rev. E **67**, 036404 (2003).
[9] A. V. Ivlev *et al.*, Phys. Rev. Lett. **90**, 055003 (2003).
[10] J. Goree, G. E. Morfill, V. N. Tsytovich, and S. V. Vladimirov, Phys. Rev. E **59**, 7055 (1999).
[11] G. E. Morfill *et al.*, Phys. Rev. Lett. **83**, 1598 (1999).
[12] D. Samsonov and J. Goree, Phys. Rev. E **59**, 1047 (1999).
[13] M. Mikikian and L. Boufendi, Phys. Plasmas **11**, 3733 (2004).
[14] H. Rothermel, T. Hagl, G. E. Morfill, M. H. Thoma, and H. M. Thomas, Phys. Rev. Lett. **89**, 175001 (2002).
[15] E. Thomas, Jr., B. M. Annaratone, G. E. Morfill, and H. Rothermel, Phys. Rev. E **66**, 016405 (2002).
[16] G. E. Morfill *et al.*, Phys. Rev. Lett. **92**, 175004 (2004).
[17] S. A. Khrapak, A. V. Ivlev, G. E. Morfill, and H. M. Thomas, Phys. Rev. E **66**, 046414 (2002).
[18] A. A. Mamun, P. K. Shukla, and R. Bingham, Phys. Lett. A **298**, 180 (2002).
[19] D. Jovanović and P. Shukla, Phys. Lett. A **308**, 369 (2003).

[20] A. Lipaev *et al.* (in preparation).
[21] G. Morfill, S. Zhdanov, and the PKE-Nefedov team, *Trampoline Effect*, Second PKE-Nefedov symposium, October, 2002, Garching, Germany (unpublished).
[22] S. I. Popel *et al.*, Phys. Rev. E **67**, 056402 (2003).
[23] S. A. Khrapak, A. V. Ivlev, S. K. Zhdanov, and G. E. Morfill, Phys. Plasmas **12**, 042308 (2005).
[24] L. S. Frost, Phys. Rev. **105**, 354 (1957).
[25] S. Ratynskaia *et al.*, Phys. Rev. Lett. **93**, 085001 (2004).
[26] V. E. Fortov, A. G. Khrapak, S. A. Khrapak, V. I. Molotkov, and O. F. Petrov, Usp. Fiz. Nauk **174**, 495 (2004) [Phys. Usp. **47**, 447 (2004)].
[27] A. V. Zobnin, A. P. Nefedov, V. A. Sinel'shchikov, and V. E. Fortov, JETP **91**, 483 (2000).
[28] M. Lampe, V. Gavrishchaka, G. Ganguli, and G. Joyce, Phys. Rev. Lett. **86**, 5278 (2001); M. Lampe *et al.*, Phys. Plasmas **10**, 1500 (2003).
[29] S. A. Khrapak, A. V. Ivlev, G. E. Morfill, and S. K. Zhdanov, Phys. Rev. Lett. **90**, 225002 (2003).
[30] S. A. Khrapak *et al.*, IEEE Trans. Plasma Sci. **32**, 555 (2004).
[31] A. V. Ivlev, S. A. Khrapak, S. K. Zhdanov, G. E. Morfill, and G. Joyce, Phys. Rev. Lett. **92**, 205007 (2004).
[32] A. V. Ivlev, S. K. Zhdanov, S. A. Khrapak, and G. E. Morfill, Plasma Phys. Controlled Fusion **46**, B267 (2004).
[33] A. V. Ivlev, S. K. Zhdanov, S. A. Khrapak, and G. E. Morfill, Phys. Rev. E **71**, 016405 (2005).